Manuscript Details

Manuscript number	JCOMB_2017_307_R5
Title	DAMAGE CHARACTERIZATION OF STIFFENED GLASS-EPOXY LAMINATES UNDER TENSILE LOADING WITH ACOUSTIC EMISSION MONITORING
Article type	Full Length Article

Abstract

The design of composite components in the aerospace industry often includes structural discontinuities, such as cutouts, for functional requirements like ventilation, tunnel passage, maintenance and repair. The presence of cutout holes leads to complicated stress concentrations with a substantial reduction in structural stability and strength of the resulting composites. It is known that reinforcing with additional material at the cutout zones can extend the damage tolerance of a structure, therefore maintaining structural integrity and load carrying capacity. This study focuses on the experimental investigation of the tensile behavior and failure characteristics of stiffened glass/epoxy composite laminates, with cutouts, under acoustic emission monitoring. The progressive failure mechanisms of laminates with cutouts and the potential benefits of additionally dropped reinforcements are evaluated under tensile loading. The additional reinforcements were provided in either a step-like or as a simultaneous drop-off sequence between adjacent continuous plies. Results showed that adding ply drop reinforcements at the location of the cutout hole improves the stiffness, strength, and also prolongs the life of the composite laminates. It is also observed that step-like ply drop arrangements performed more effectively than simultaneously dropped configurations. The location and extent of damage identified by microscopic images correlated well with the acoustic emission results.

Keywords	A. Glass fibers; B. Mechanical properties; D. Acoustic emission; Cutout hole effect
Manuscript region of origin	Europe

Corresponding Author	Carlo Santulli
Corresponding Author's Institution	Università di Camerino
Order of Authors	arumugam v, K Saravanakumar, Carlo Santulli
Suggested reviewers	Fabrizio Sarasini, Claudio Scarponi

Submission Files Included in this PDF

File Name [File Type]

cover_letter_arumugam13.doc [Cover Letter]

answer_arumugam13.doc [Response to Reviewers]

20_Main Text Fig Stiff Tensile behaviour_rev Corrected.docx [Manuscript File]

To view all the submission files, including those not included in the PDF, click on the manuscript title on your EVISE Homepage, then click 'Download zip file'.

Carlo Santulli
Associate Professor in Materials Science and Technology
Viale della Rimembranza
63100 Ascoli Piceno, Italy
E-mail: carlo.santulli@unicam.it

26th January 2017

I am here introducing the paper "Damage characterization of stiffened glass-epoxy laminates under tensile loading with acoustic emission monitoring", which we are submitting to be considered for publication in Composites Part B.

This paper is concerned about the design of composite components in the aerospace industry, which often includes structural discontinuities, such as cutouts, for functional requirements like ventilation, tunnel passage, maintenance and repair. The presence of these cutout holes leads to complicated stress concentrations with a substantial reduction in structural stability and strength of the resulting composites. It is known that reinforcing with additional material at the cutout zones can extend the damage tolerance of a structure, which is an efficient method to maintain structural integrity and load carrying capacity. This study focuses on the experimental investigation of the tensile behavior and failure characteristics of stiffened glass/epoxy composite laminates, with cutouts, under acoustic emission monitoring. The progressive failure mechanisms of laminates with cutouts and the potential benefits of additionally dropped reinforcements are evaluated under tensile loading. The additional reinforcements were provided in either a step-like or as a simultaneous drop-off sequence between adjacent continuous plies. Results showed that adding ply drop reinforcements at the location of the cutout hole improves the stiffness, strength, and also prolongs the life of the composite laminates. It is also observed that step-like ply drop arrangements performed more effectively than simultaneously dropped configurations. The location and extent of damage identified by microscopic images correlated well with the acoustic emission results.

This work is in the frame of long time collaboration, started back in 2009, between two groups active in acoustic emission on composites and impact damage assessment, led respectively by myself and Dr. Arumugam in Chennai University (India), which produced already a number of joint papers. These include:

1. Suresh Kumar C, Arumugam V, Santulli C, Characterization of indentation damage resistance of hybrid composite laminates using acoustic emission monitoring, Composites Part B 111, 2017, 165-178.
2. Jefferson AJ, Arumugam V, Santulli C, Effect of post-cure temperature and different reinforcements in adhesive bonded repair for damaged glass/epoxy composites under multiple quasi-static indentation loading, Composite Structures 143, 2016, 63-74.
3. Jefferson AJ, Arumugam V, Santulli C, Jennifers A, Poorani M, Failure modes in fiberglass after multiple impacts: an acoustic emission and digital image correlation study, Journal of Engineering and Technology 8 (2), 2015, paper n.4.

4. Santulli C, Sajit S, Arumugam V, Failure mode discrimination in mode II fracture of glass/epoxy laminates using acoustic emission technique, Materials Science and Engineering with Advanced Research 1 (2), 2015, 16-25.
5. Jefferson Andrew J, Arumugam V, Saravanakumar K, Dhakal HN, Santulli C, Compression after impact strength of repaired GFRP composite laminates under repeated impact loading, Composite Structures 113, 2015, 911-920.
6. Kakakasery J, Arumugam V, Abdul Rauf K, Bull D, Chambers AR, Scarponi C, Santulli C, Cure cycle effect on impact resistance under elevated temperatures in carbon prepreg laminates investigated using acoustic emission, Composites Part B 75, 2015, 298–306.
7. Arumugam V, Adhithya Plato Sidharth A, Santulli C, Characterization of failure modes in compression-after impact of glass–epoxy composite laminates using acoustic emission monitoring, Journal of the Brazilian Society of Mechanical Sciences and Engineering 37 (5), 2015, 1445-1455.
8. Arthurs B, Bull DJ, Arumugam V, Chambers AR, Santulli C, Porosity effect on residual flexural strength following low energy impact of carbon fibre composites, Polymers and Polymer Composites 23, 2015, 205-212.
9. Suvarna R, Arumugam V, Bull DJ, Chambers AR, Santulli C, Effect of temperature on low velocity impact damage and post-impact flexural strength of CFRP assessed using ultrasonic c-scan and micro-focus computed tomography, Composites Part B 66, 2014, 58-64.
10. Dhakal HN, Arumugam V, Aswinraj A, Santulli C, Zhang ZY, Lopez-Arraiza A, Influence of temperature and impact velocity on the impact response of jute/UP composites, Polymer Testing 35, 2014, 10-19.
11. Balan R, Arumugam V, Abdul Rauf K, Adhithya Plato Sidharth A, Santulli C, Estimation of residual flexural strength of unidirectional GFRP composite laminates under repeated impact load, Journal of Composite Materials 49, 2014, 713-722.
12. Arumugam V, Adhithya Plato Sidharth A, Santulli C, Failure modes characterization of impacted CFRP laminates under compression loading using acoustic emission, Journal of Composite Materials 48, 2013, 3457-3468.
13. Boominathan R, Arumugam V, Santulli C, Adhithya Plato Sidharth A, Anand Sankar R, Sridhar BTN, Acoustic emission characterization of the temperature effect on falling weight impact damage in carbon/epoxy laminates, Composites Part B 56, 2014, 891-898.
14. Arumugam V, Kumar S, Santulli C, Sarasini F, Stanley AJ, Identification of failure modes in composites from clustered acoustic emission data using pattern recognition and wavelet transformation, Arabian Journal for Science and Engineering 38 (5), 2013, 1087-1102.
15. Asokan R, Arumugam V, Santulli C, Barath Kumar S, Joseph Stanley A, Acoustic emission monitoring of repaired composite laminates, Journal of Reinforced Plastics and Composites 31(18), 2012, 1226-1235.
16. Asokan R, Arumugam V, Santulli C, Barath Kumar S, Joseph Stanley A, Investigation of the strength of the failure modes in GFRP laminates using acoustic emission monitoring, International Journal of Polymers and Technologies 3 (2), 2011, 57-65.
17. Arumugam V, Kumar S, Santulli C, Stanley AJ, Effect of fiber orientation in unidirectional glass epoxy laminate using acoustic emission monitoring, Acta Metallurgica Sinica (English letters) 24 (5), 2011, 351-364.
18. Arumugam V, Kumar S, Santulli C, Sarasini F, Stanley AJ, A global method for the identification of failure modes in fibreglass using acoustic emission, Journal of Testing and Evaluation 39 (5), 2011, 103730.

I respectfully trust that this paper will be of interest for both the reviewers and the journal's readers and am therefore submitting it to your attention. Kind regards

Carlo Santulli

Reviewer 1

The paper can be accepted for publication.

Reviewer 3

The paper can be accepted to publication

There are no required edits, therefore the paper has been just modified by taking off the yellow highlights and correcting a few typos.

DAMAGE CHARACTERIZATION OF STIFFENED GLASS-EPOXY LAMINATES UNDER TENSILE LOADING WITH ACOUSTIC EMISSION MONITORING

V. Arumugam, * [1], K. Saravanakumar,[1] C. Santulli[2]

[1] Department of Aerospace Engineering, Madras Institute of Technology, Anna University, Chennai, India

[2] School of Architecture and Design, Università di Camerino, Ascoli Piceno, Italy

Abstract

The design of composite components in the aerospace industry often includes structural discontinuities, such as cutouts, for functional requirements like ventilation, tunnel passage, maintenance and repair. The presence of cutout holes leads to complicated stress concentrations with a substantial reduction in structural stability and strength of the resulting composites. It is known that reinforcing with additional material at the cutout zones can extend the damage tolerance of a structure, therefore maintaining structural integrity and load carrying capacity. This study focuses on the experimental investigation of the tensile behavior and failure characteristics of stiffened glass/epoxy composite laminates, with cutouts, under acoustic emission monitoring. The progressive failure mechanisms of laminates with cutouts and the potential benefits of additionally dropped reinforcements are evaluated under tensile loading. The additional reinforcements were provided in either a step-like or as a simultaneous drop-off sequence between adjacent continuous plies. Results showed that adding ply drop reinforcements at the location of the cutout hole improves the stiffness, strength, and also prolongs the life of the composite laminates. It is also observed that step-like ply drop arrangements performed more effectively than simultaneously dropped configurations. The location and extent of damage identified by microscopic images correlated well with the acoustic emission results.

Keywords: A. Glass fibers; B. Mechanical properties; D. Acoustic emission; Cutout hole effect

* Corresponding author. E-mail address: arumugam.mitaero@gmail.com (Arumugam V).

1. Introduction

The evolution of fiber reinforced plastic (FRP) composites has developed new vistas in aerospace industries. Primary structural components, such as wings, fins, helicopter rotor blades, stiffened structures with joints and access holes, etc., are fabricated by the termination of internal ply-drop off to enhance weight reduction, cost effectiveness, and obtain tailored stiffness values. The mechanical behavior of the composite structure is drastically affected due to the presence of cutouts, such as access holes for hydraulic piping, electrical wiring and fastener holes, which become critical during loading conditions [1]. It is crucial to have a sound and complete idea of the intricate behavior around notched areas, connecting the bolts and rivets [2]. High stresses are produced around holes because of material discontinuities causing a relatively larger reduction in strength than unnotched laminate [3-6]. Takeda et al. studied the tensile behavior of glass/epoxy plain weave fabric-reinforced laminates under cryogenic temperatures investigating the progressive failure methodology [7]. Kaltakci [8] studied the effects of fiber orientation and stress concentration on single-layered anisotropic plates with/without holes, revealing significant influence on the fracture behavior based on 3D weaving of different bundle size of the yarns. Aljibori et al. [9] investigated the compressive behavior of woven glass fiber/epoxy composite laminate plates with and without a cutout. The effect of cutout size and fiber orientation angle has also been considered, in models predicting strength and damage accumulation in open hole composite laminates with different failure criteria [10-12]. Observations unveiled the fact that cross-ply orientation possesses higher strength than other fiber orientations. Also, as the cutout size increases, load bearing capacity decreases due to the effect of material discontinuities.

Murat Arslan et al. investigated the stress analysis of isotropic and orthotropic plates with and without cutout hole using finite element methods [13]. Camanho et al. proposed a fracture mechanics model based on unnotched specimen strength and fracture toughness, for predicting open hole tensile (OHT) strength of composite laminates [14]. Lee and Kim studied compressive response and damage evolution in laminated plates with cutouts based on a micromechanical constitutive model [15]. The damage was found to be controlled by the interfacial fiber debonding and nucleation of microcracks in the matrix. The employed model predicted accurately results for cross-ply, while it overestimated stiffness and failure load for angle-ply and quasi isotropic plates. Several studies employed computational FEM models for predicting

tensile strength and progressive damage in notched composite laminates [16-20]. Chen et al. [16] employed smeared crack model using cohesive element to investigate the scaling effects on open hole tension testing on composite laminates which correlated well with the experimental results by Wisnom et al. and Hallett et al. [17-18]. Ridha et al. studied the prediction of ultimate open hole (OHT) strength and failure progression of notched laminates with various size and stacking sequence based on progressive damage model with initial in-plane damage and delamination [19]. Maa and Cheng were able to predict failure strength and load–deflection relations of notched laminated composites, again discussing the effects of hole size and specimen width [20].

Ersin et al. studied the effect of circular hole location on lateral buckling of woven composite laminates [21]. Predominant failure mode, i.e., delamination, grows significantly because of interlaminar stress at the free edges [22]. To prevent such stress concentrations around the cutout holes and to avoid strength reduction, suitable reinforcements must be installed around the cutout regions to improve sufficient load bearing capacity of laminates [23]. Being a damage prone region, it is advisable to monitor the progression of failure and onset location of delamination to forecast the damage.

Acoustic emission, as a structural monitoring technique, proved able to detect microscopic failure events under loading conditions. A number of studies have been carried out for the identification of the failure modes in damaged composite materials e.g., post-impact loading, using parametric-based approach and signal-based approach [24-26]. In particular, several studies utilized AE parametric approach to characterize the damage mechanism based on AE parameters, such as amplitude, counts, duration, energy and rise time, to determine the nature of failure and the location of emission source [27-29]. Berthelot et al. employed AE parametric approach to discriminate failure modes in different stacking sequences (0°, 0°/90°, 0°/45°, 90°/45°) [30]. Different failure modes encountered in composites are matrix cracking, fiber-matrix debonding, delamination and fiber breakage [31-33]. These failure events cause transient, elastic stress waves, which can be detected by piezoelectric sensors attached to the composite structure using suitable couplant. The damage mechanisms of self-reinforced polyethylene (SRPE) during tensile loading have been investigated by Zhuang et al. [34], in which case acoustic emission signals and amplitude histogram plots were associated with SEM images depicting the nature of damage. Ramirez-Jimenez et al. [35] and Arumugam et al. [36]

investigated the classification of failure modes based on the primary frequency content of AE signals. They also discussed the discrimination of failure modes based on signals' amplitude, concluding that the AE signals associated with low amplitudes and low duration are related to matrix cracking, those with moderate amplitude and duration are related to fiber-matrix interface debonding and those with medium to high amplitude are associated with fiber breakage. Similarly, Kotsikos et al. investigated the different failure mechanisms in glass/epoxy laminates under fatigue loading. They reported that the low amplitude signal range (from 40 to 55 dB) is related to matrix cracking, the medium range (from 55 to 70 dB) is associated with interfacial debonding and high amplitude signals (>70 dB) belong to fiber breakage [37].

This study focuses on the uni-axial tensile behaviour and failure characteristics of GFRP laminates with cut-outs. Its aim is particularly linked to the fact that the effectiveness of cutouts, not leading to extensive damage, which can also be applied when repair is needed since the procedure is basically the same, has been only limitedly investigated with acoustic emission. What is suggested is that the remediation after the creation of cut-outs may change the mode of damage in the composites. More specifically, acoustic emission can offer indications in cases where two different repair modes are possible on the respective suitability for mechanical remediation of the composites, of course till the extent this is possible. Since repair enhances and extends the life of composites, this is a crucial topic very limitedly studied so far with acoustic emission, as suggested from literature.

The influence of additional reinforcements at the location of cut-out has also been discussed. It is observed that reinforcing with additional material at cut-out zones can extend the damage tolerance of structure, maintaining on the other side structural integrity and load carrying capacity. The mechanism of damage progression and various failure modes during loading have been investigated using acoustic emission monitoring.

2. Materials and Methods

2.1 Fabrication of conventional E-glass/epoxy laminates

The laminate consists of 12 layers of unidirectional E-glass fiber mat with an areal weight of 220 g/m^2 and epoxy resin (Araldite LY556) at a ratio of 1:1 by weight. The resin was mixed with the hardener (HY951) at a ratio of 10:1 by weight, to accelerate the curing process. The resin was

allowed to impregnate the reinforcement with the aid of rollers. The fabricated laminate has a stacking sequence $[0°]_{12}$ yielding a nominal thickness of 3.5 (±0.15) mm. The laminate was fabricated by hand lay-up technique. **ASTM D3039** tensile test specimens of dimension 280 mm long, 30 mm wide were cut from the laminates using abrasive water jet cutting.

2.2 Fabrication of laminates with submerged plies as cutout reinforcement

These laminates were fabricated with the experimental procedure similar to that of conventional laminates, exposed in Section 2.1. Additional ply reinforcements were dropped off at the center during the hand layup process, which were supposed to enhance the strength and integrity of the cutout hole. The plies were dropped off in different stacking arrangements, namely step-like and simultaneous between adjacent covering continuous plies, as shown in Figure 1. Both the step-like and the simultaneous configuration have the same ply arrangement as $\mathbf{[0°_2\ /\underline{0°}/0°/\underline{0°}\ /0°/\underline{0°}\ /0°_2]_S}$ within which the underlined plies indicate the dropped submerged reinforcements. In the step-like arrangement, the plies were dropped with a stagger distance of 5 (±0.5) mm. In contrast, in the simultaneous arrangement, the plies were dropped instantaneously at the same station between the adjacent covering plies, as suggested in [38]. As a whole, six additional reinforcement plies were introduced between adjacent plies. A total of 18 plies were used therefore for fabricating cutout reinforced laminates. Only [0°] plies were used for all the dropped and covering ply configurations. The fabricated laminate has a nominal thickness of 3.5 (±0.15) mm and 4.5 (±0.25) mm in thin and thick section, respectively. Initially, the plies were marked for placement of additional reinforcement to avoid misalignment. Also in this case, **ASTM D3039** tensile test specimens of dimension 280 mm long, 30 mm wide were cut from the laminates using abrasive water jet cutting.

In particular, some guidelines from Varughese et al. [38] were followed, such as:

- Dropping only one single ply at each station
- Plies must be dropped with stagger distance
- Each dropped ply must be covered with adjacent continuous/belt plies to minimize the delamination at the junction of terminated ply drop. This has been followed to reduce stress concentration to a great extent by distributing dropped plies over a region at

specific locations. Severe geometric profile change can also be avoided by dropping plies gradually.

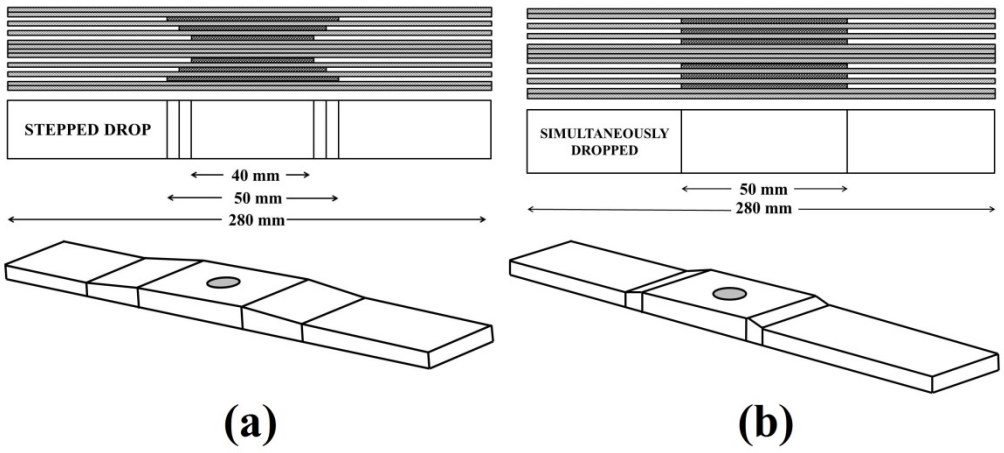

Figure 1. (a) Type III & IV Stepped Drop configuration and (b) Type V & VI Simultaneous Drop configuration

Type I	Conventional laminate without hole
Type II	Conventional laminate with 10 mm hole
Type III	Stepped drop configuration laminate without hole
Type IV	Stepped drop configuration laminate with 10 mm hole
Type V	Simultaneous drop configuration laminate without hole
Type VI	Simultaneous drop configuration laminate with 10 mm hole

Table 1 Codes of different Types of specimens for Tensile testing.

3. Experimental Procedure

3.1 Tensile testing under acoustic emission monitoring

The fabricated specimens were subjected to monotonic uniaxial tensile test. The upper and lower edges of the specimens were clamped to the tensile fixture of Tinius Olsen universal testing machine with a load-cell capacity of 100 kN. The crosshead speed of the machine was fixed to 0.5 mm/min. The test was performed at ambient environmental conditions. Tensile testing of glass/epoxy specimens was performed according to ASTM D3039 standards. Five

specimens were tested in all categories and their averages were considered. Online acoustic emission monitoring was carried out using an eight channel AE setup supplied by Physical Acoustics Corporation. Acoustic signals were continuously monitored by using a SAMOS E3.10 data acquisition system with a sampling rate of 3 MSPS and a 40 dB pre-amplification. Ambient noise was filtered using a threshold of 45 dB. To improve the acoustic transmission, a couplant is applied between the contact surface of the specimen and AE sensor. The source location of AE events was evaluated from the difference in the arrival time of the AE signals received by the two sensors. The signal definition times used for AE monitoring were as follows: Peak Definition Time (PDT)=21 μs, Hit Definition Time (HDT)= 160 μs and Hit Lockout Time (HLT)= 300 μs. Furthermore, two wide band sensors with 100-900 kHz frequency were symmetrically attached to the tensile specimens at the gauge sections to monitor the failure mechanism and damage locality during tensile loading, as shown in Figure 2. Code of different Types of glass/epoxy specimens considered in this study is summarized in Table 1. Henceforth these codes will be mentioned to discuss the tensile behavior and damage mechanisms of various Types of specimens.

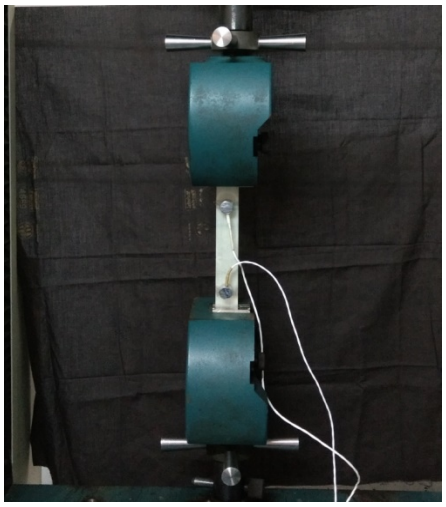

Figure 2. Tensile specimens with acoustic emission sensors fitted

4. RESULTS AND DISCUSSION

4.1 Mechanical tests

In this study, the effects of circular cutouts and the influence of additional submerged reinforcements as strength bearing plies with two different ply-drop sequences in glass/epoxy laminates under the uni-axial tensile loading have been experimentally investigated. The tensile response has been summarized in Figure 3, as far as ultimate load and ultimate displacement are concerned. The comparison is between laminate Types with no holes (I, III and V) and those with 10 mm holes (II, IV and VI), in the understanding that hole produces some reduction in the performance of laminates, yet repair is aimed to compensate for this reduction: the expected positive effects of the two repair procedures applied (stepped drop or simultaneous drop) are compared. As a preliminary consideration, results from Figure 3 indicate that both repair procedures are effective, although stepped drop offered considerably higher performance than simultaneous drop. The difference between the two procedures is much more evident in the case of time needed for failure, as it is shown in Table 2.

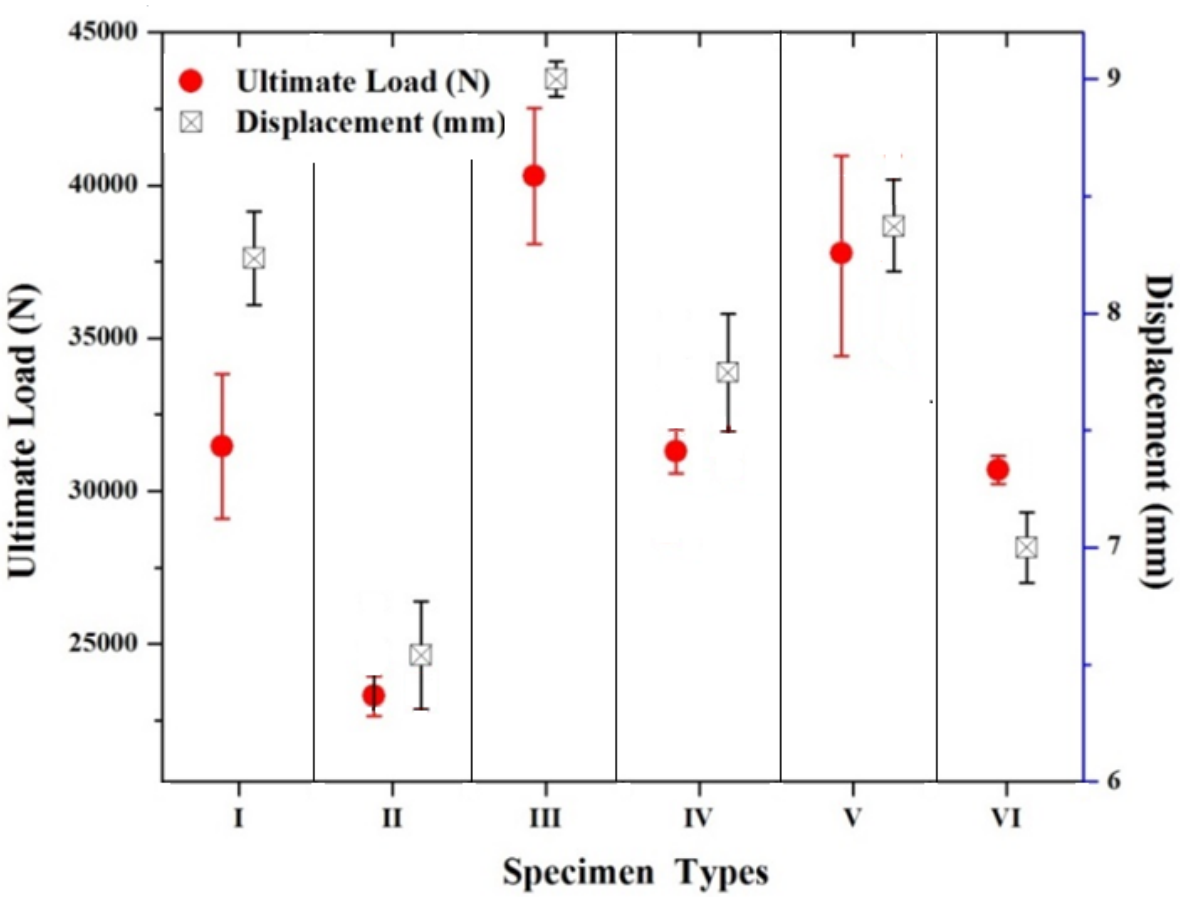

Figure 3. Ultimate load and maximum displacement plot

Laminate Type	Failure time (s)
I	510 ± 11
II	284 ± 6
III	539 ± 11
IV	474 ± 6
V	499 ± 5
VI	366 ± 39

Table 2 Failure time for the different types of laminates

In practice, the insertion of additional submerged plies at the zones of cutouts acts as a stress reducer and enhances the strength and load bearing capacity of the laminates, an effect which is visible from the results. Type III & Type IV laminates utilized a stepped ply drop configuration for stacking arrangement. The stagger distance of 5 mm between each drop ply was deemed to introduce ply drop stations and resin rich zones, which may act as stress raisers to cause premature failure. These drop zones are observed to be critical in Type V & Type VI laminates, since sudden tapering results in more resin-rich zones and earlier failure of specimens. It can be therefore acknowledged that influence of additional ply reinforcements into the zones of cutout location enhances effective load bearing capacity and strength in composite laminates.

Figure 4(a) & 4(b) show percentage strength improvement plot due to repair either by stepped ply configuration or by simultaneous drop configuration and percentage strength reduction plot due to cutout of various laminate types, respectively. Type I undamaged laminate has a maximum average strength of 296 MPa, which can be considered as a reference for comparing the results with the other configurations. Premature damage initiation in Type II laminate in which a hole was drilled occurred due to severe stress concentrations around the cutout boundary resulting in early failure. From Figure 4(b), the maximum strength of the Type II laminates is observed to be 222 MPa, which is around 25% lesser than that of Type I laminates. In all the laminates with cutout-hole, the presence of the hole contributes to orient the location of damage and their failure was observed to be drastic and sudden. As a consequence, the scattering of tensile data obtained is quite high, which suggests the need for further analysis to better characterize damage, of which analysis acoustic emission is an example.

Overall from the tensile test results, it is seen nonetheless that Type III and Type IV laminates show potentially more strength, high strain to failure, and delay in failure time in comparison with other laminate configurations.

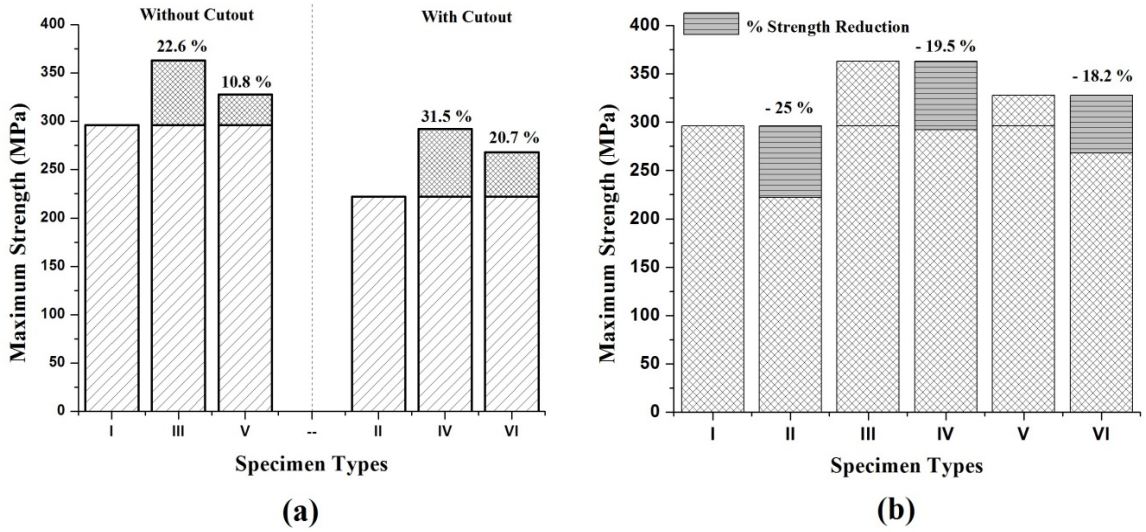

Figure 4. (a) Percentage strength improvement plot due to the two repair procedures (stepped ply drop or simultaneous ply drop) and (b) Percentage strength reduction plot as an effect of the cutout-hole

4.2 Tensile behavior of glass/epoxy specimens monitored by acoustic emission

The objective of characterizing damage outline and different failure mechanisms is to evaluate the structural performance of composite laminates. The acoustic emission technique has been implemented to monitor the progressive damage during tensile testing, characterizing the different failure mechanisms. These have been evaluated with various AE parameters, such as energy, cumulative counts, peak frequency, amplitude and events.

In particular, Figure 5 depicts the load vs. time curve with AE cumulative counts and AE energy plot for all laminate types. The initiation of AE activity occurs generally at around 100 seconds during the tensile loading. The rate of incoming AE cumulative counts was considered to be almost flat during the initial stage of load-displacement plot, which in composites is typically associated with low AE energy failure modes with amplitudes around 50–60 dB, particularly matrix cracking [39]. However, during the middle stage of load-displacement plot, intensification and fluctuation of AE cumulative counts and AE energy can be associated with interfacial failures, such as fiber debonding and pullout, the latter associated also with amplitudes greater than 80 dB, since it leads to fiber breakage. Later on, at the proximity of ultimate failure load, AE energy increases remarkably with a steep rise in the slope of cumulative counts related to

high amplitude signals representing longitudinal fiber breakage. This change of behavior can be associated with the onset of a “knee” along the AE cumulative counts curve [24], which in this case can be observed to occur at lower loads for laminates with cutout hole. Some cases are discussed also into more detail: in particular, Figure 5 (b) depicts the load vs. displacement curve with AE cumulative counts and AE energy plot for Type II conventional glass/epoxy laminates with a cutout hole. It can be observed that the tensile behavior of Type II is quite similar to the one of Type I laminate. However, microscopic damage initiation at the vicinity of cutout appears during loading at around 60% of ultimate stress, hence in advance with respect to what occurs in the Type I laminate. AE activity is limited to low intensity events during this stage, which have been related to matrix cracking. At a load of 15000 N, at about 200 s, there is a steep increase in AE cumulative counts with high intensity of AE energy, resulting in the initiation of longitudinal splitting crack at the boundary of cutout hole, which can also be seen from Figure 7. In contrast, in the case of Type III laminates, the rate of AE cumulative counts, as from Figure 5 (c), was found to be almost flat during this stage of the load-displacement plot, which has been associated with low AE energy failure mode, hence matrix cracking. At higher loads, fiber breakage took place at the free edge and at the ply-drop zones of submerged additional plies, which caused the ultimate failure of Type III laminate, as observable from Figure 8. More specifically, fiber splitting occurred on the gauge section of the laminate and progressively grew towards the submerged additional plies and then the gripping zone. Similarly, from Figure 5 (f), it can be illustrated that AE activity, though initiating once again around 100 s during tensile loading, considerably intensifies during the middle phase of loading, with strong fluctuations in AE energy and a steep rise in cumulative counts, denoting macroscopic damage initiation at the boundary of cutout hole (see also Figure 9). Furthermore, during the final stage of loading, AE energy increased remarkably, resulting in ultimate failure of laminates together with high amplitude (>80 dB) events, representing the longitudinal fiber breakage associated with other lower amplitude failure modes, such as matrix cracking and interfacial debonding/delamination.

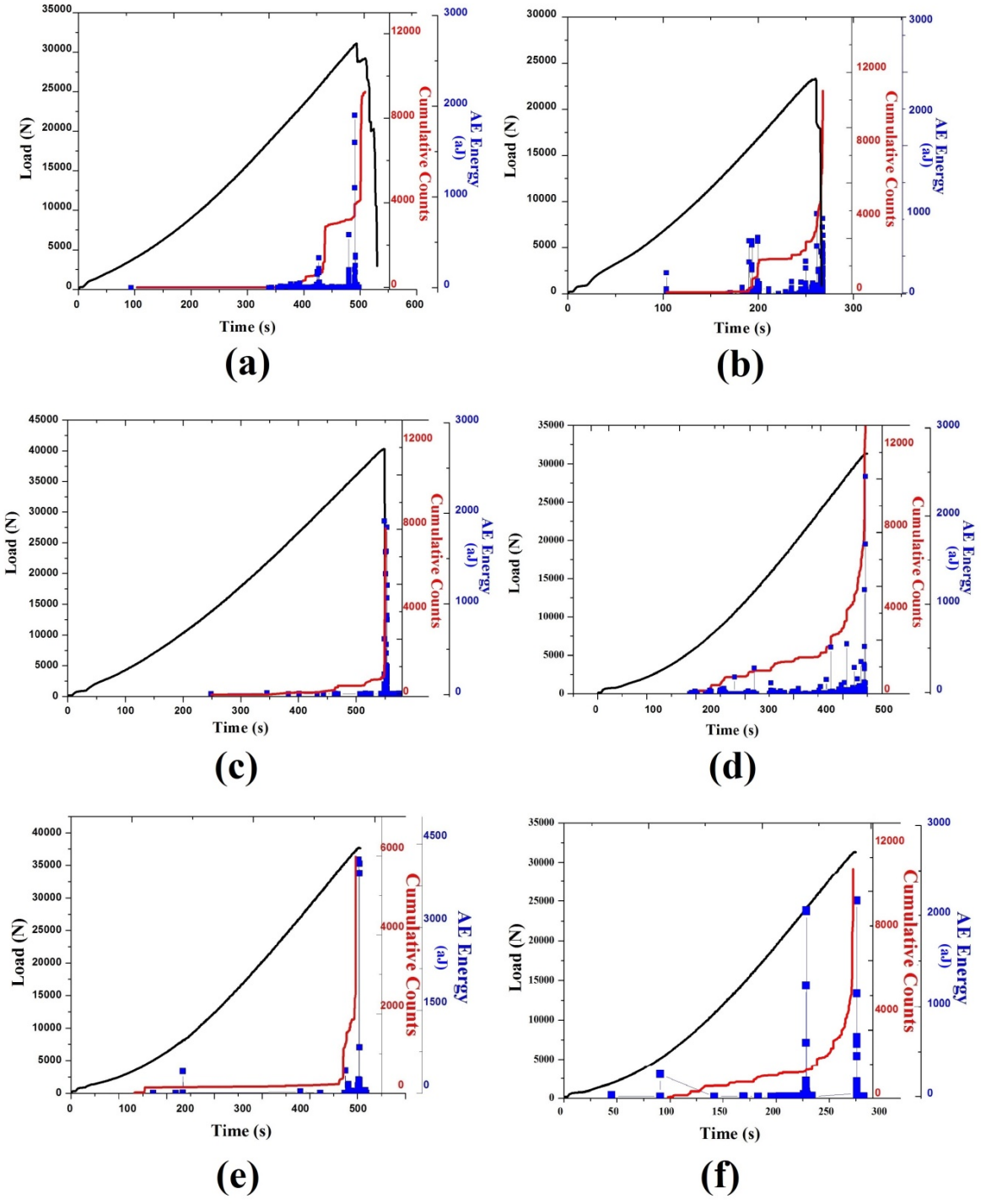

Figure 5. Load vs. Time plot with AE cumulative counts and energy of different laminates: (a) Type I (b) Type II (c) Type III (d) Type IV (e) Type V (f) Type VI

Frequency analysis was also used as an effective tool for damage characterization, as it is often the case on AE studies on composites [40], and was associated in Figure 6 to amplitude vs. location plots only on laminates with cutout holes, to investigate the effect of the hole on AE activity. To summarize, the frequencies of AE events detected can be tentatively categorized into four ranges, 90-170, 200-270, 270-300 and 310-360 kHz, respectively related to different failure modes, matrix cracking, debonding, delamination and fiber breakage. Figure 6 (a) shows peak frequency vs. time plot for Type II laminates. It is observed that the contribution to matrix cracking damage is higher. However, the central frequency ranges, associated to debonding and delamination, are typically developed at the vicinity of cutout hole, whereas high frequency events related to fiber breakage take place during the ultimate failure. Figure 6 (b) depicts amplitude vs. location plot for Type II specimens. Here the distribution of AE signals was concentric around the cut-out hole. The failure initiation has occurred with low amplitude matrix cracking signals (40–55 dB), originating at the zones of cutout hole. Furthermore, events in the moderate amplitude range (55–70 dB) can be attributed to the onset of significant debonding and delamination. Finally, the amplitude signals beyond 70 dB are supposed to be related to fiber failure, which is often encountered in literature on AE studies on composites [36, 41]. In general, initiation of AE events during the testing brings out all the failure phenomena. Comparing Figure 6 (a) and (b), it is observed that the AE events were centralized at the vicinity of cutout, yet fiber breakage only takes place in a very abrupt and critical way at the very end of loading, leading to ultimate failure. Figure 6 (c) depicts the peak frequency vs. time plot for Type IV laminate, the frequency intervals obtained were very similar to Type II ones, but the intensity of various failure modes was different: in particular AE signals pertaining to matrix cracking peak frequency range initiated very soon after loading started. However, debonding and delamination were the predominant failures mode in Type IV laminates. The concentration of these signals was enormous due to failure at the zone of ply-drop (resin-rich zones), resulting in premature delamination. Similarly, fiber breakage signals were also in a larger amount compared to the Type II laminates, because of local fiber failure at additional cutout reinforcements, which can be seen from Figure 8. This difference is confirmed by amplitude vs. location plot for Type IV laminate, shown in Figure 6 (d). Here, the distribution of signals was different from Type II with less intense AE signals at the boundary location of the cutout, but rather dispersed over a region. This was explained by the introduction of additional ply reinforcements resulting in further

interfacial failure modes, such as debonding and delamination, which is relevant to moderate amplitude ranges. In other words, Type IV laminate with additional submerged reinforcements in a step-like ply arrangement acts as a damage constraining configuration at the zones of cutout hole, therefore delaying damage initiation. The initiation of damage only occurred at a level of around 85% of ultimate load in Figure 8, similarly to what occurred in Type I & III laminates with no holes. This delay in failure is because of stress redistribution through the additional reinforcements at the zones of the hole. Figure 6 (e) depicts the peak frequency vs. time plot for Type VI laminates. The frequency intervals obtained for Type II/IV/VI laminates were very similar, but the intensity of failure modes was different in each case. In particular, in laminates with holes AE signals pertaining to matrix cracking initiated from the beginning of the loading. However, debonding and delamination were predominant failure modes in Type IV and Type VI laminates. The dispersion of these signals was more due to the presence of resin rich zone near ply-drop resulting in premature delamination. This can be evident from Figure 9 showing failure stages of Type V & VI laminates, where the ultimate failure occurred in the drop zone of additional ply reinforcements.

Figure 6 (f) illustrates the amplitude vs. location plot for Type VI laminates, here the distribution of signals was different from that of Type II and Type IV ones. The unbalanced distribution of AE signals across the gauge length indicated that the failure occurred in the ply-drop zones. The introduction of additional ply reinforcements resulted in further interfacial failure modes, such as debonding and delamination, which is relevant to moderate amplitude ranges. Type VI laminate employs the simultaneously dropped ply configuration, leading to a sudden change in geometric profile and more resin rich zone causing premature failure. Overall, from the tensile behavior, the failure of submerged cutout reinforced laminate occurred by crack propagation and delaminated into the thick section, because of introducing high stiffness 0° dropped plies.

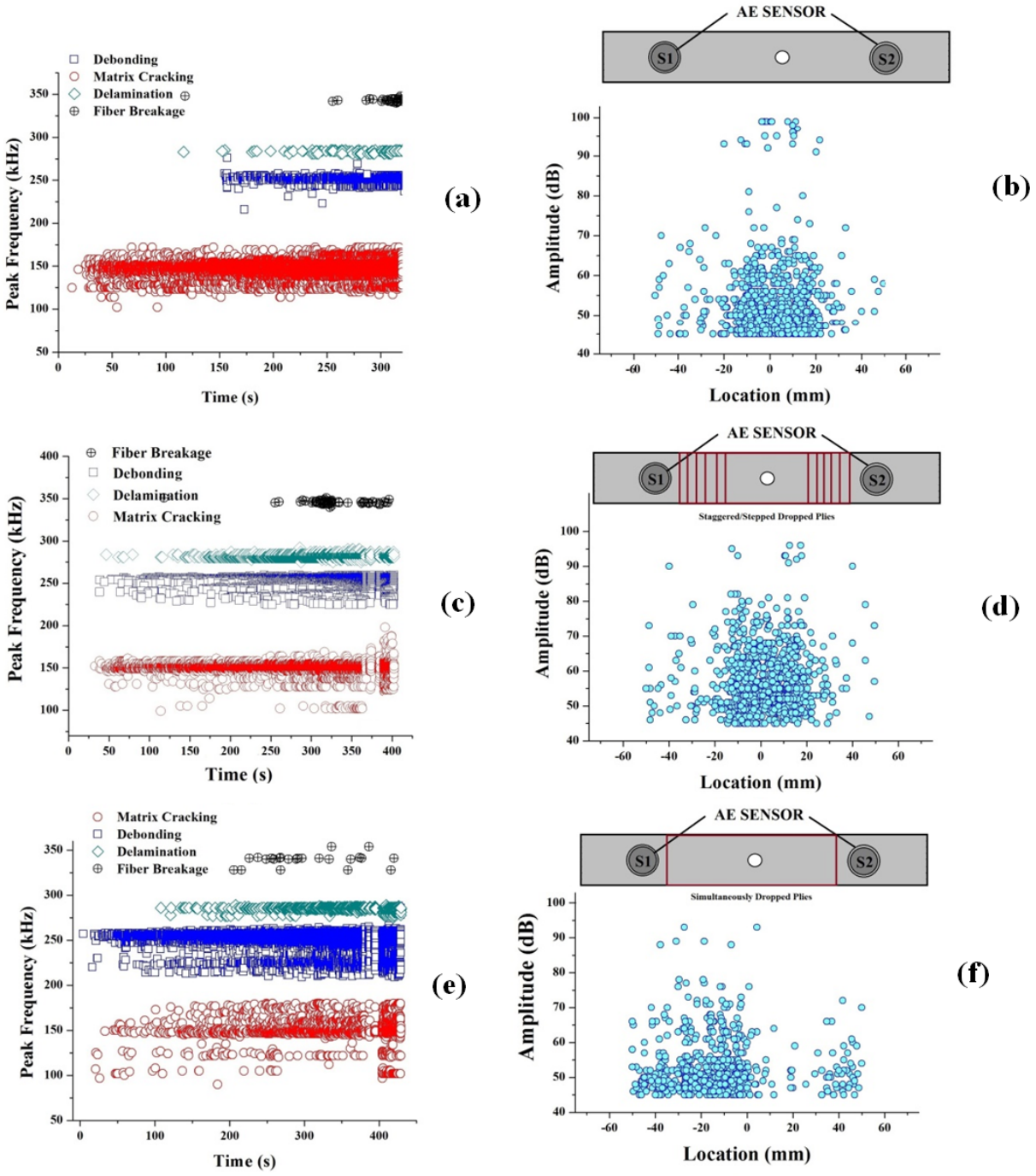

Figure 6.

Type II laminates: (a) Peak frequency vs. Time plot; (b) Amplitude vs. Location plot

Type IV laminates: (c) Peak frequency vs. Time plot; (d) Amplitude vs. Location plot

Type VI laminates: (e) Peak frequency vs. Time plot; (f) Amplitude vs. Location plot

Coming now to a global analysis of Figure 7, 8 and 9, here images at 85% and 100% of ultimate load are depicted: it was found that at a percentage of ultimate load such as 85% significant differences can be observed: in all cases, intensive matrix cracking at the location of ply-drop zones beyond the region of cutout were observed at this load level. In particular, in Type III & IV laminates, the initiation of visible damage occurred only at 85% loading, which evidenced that additional ply reinforcement enhances the structural integrity by stress redistribution. Similarly in Figure 9, the microscopic images show the fiber breakage and pullout at the ply-drop zone at 100% failure load. The ultimate failure images of Type VI specimens show the matrix cracking and delamination at the zone of sudden drop leading to fiber pullout failure. The load bearing capability of Type V & VI laminates is therefore better than it is the case for Type I & II laminates, yet poor when compared to Type III and IV ones. Type V & VI laminates enclose simultaneously dropped ply arrangement, causing local stress concentration at the drop zone. Thus the failure initiated at this location, further delayed the failure at the cutout hole, yet ultimate failure occurred at this ply-drop zones. This allows concluding that exceeding a level of additional reinforcements may give rise to local stress concentration because of change in laminate profile.

Figure 10 shows normalized AE hits of specimens with cutout deemed to correspond to different failure modes, such as matrix cracking, debonding, delamination and fiber breakage. It is observed that matrix cracking was observed to be higher in Type II laminates compared to Type IV and Type VI ones. This was explained by the presence of stress concentration around the hole in Type II laminates, initiated early intra-laminar matrix cracking during loading resulted in high intensity of matrix cracking. However, this has decreased in Type IV and Type VI specimens due to high load bearing capacity and stress redistribution through additional ply-drop arrangement. In contrast, the debonding and delamination is observed to increase in the Type IV and Type VI specimens due to the presence of resin rich zone at the vicinity of dropped ply [34]. The intensity of debonding and delamination was very high in Type VI simultaneously dropped specimen configuration than the Type IV stepped/staggered drop configuration. It is evident that the simultaneous dropped ply arrangement inhibits high local stress concentration due to sudden change in profile resulting in early failure than the Type IV step-like drop-ply configuration.

From the above discussion, the evolution of the damage pattern of the Types of laminates configurations with ply-drop arrangement during tensile testing has been considered. The failure of cutout hole specimens with additional submerged reinforcements has better structural integrity and damage tolerance than the conventional specimen with no additional submerged plies at the region of the cutout. It has clearly been revealed that introducing the additional submerged reinforcements at the regions of cutout during fabrication can reduce the possibility of damage initiation by alleviating stress concentration and enhance the strength of the specimens when compared to the Type I and II specimens. Moreover, it is more effective to reinforce the additional ply arrangements gradually than introducing them simultaneously: the reason is that this procedure enhances obtaining a uniform stress distribution between the layups.

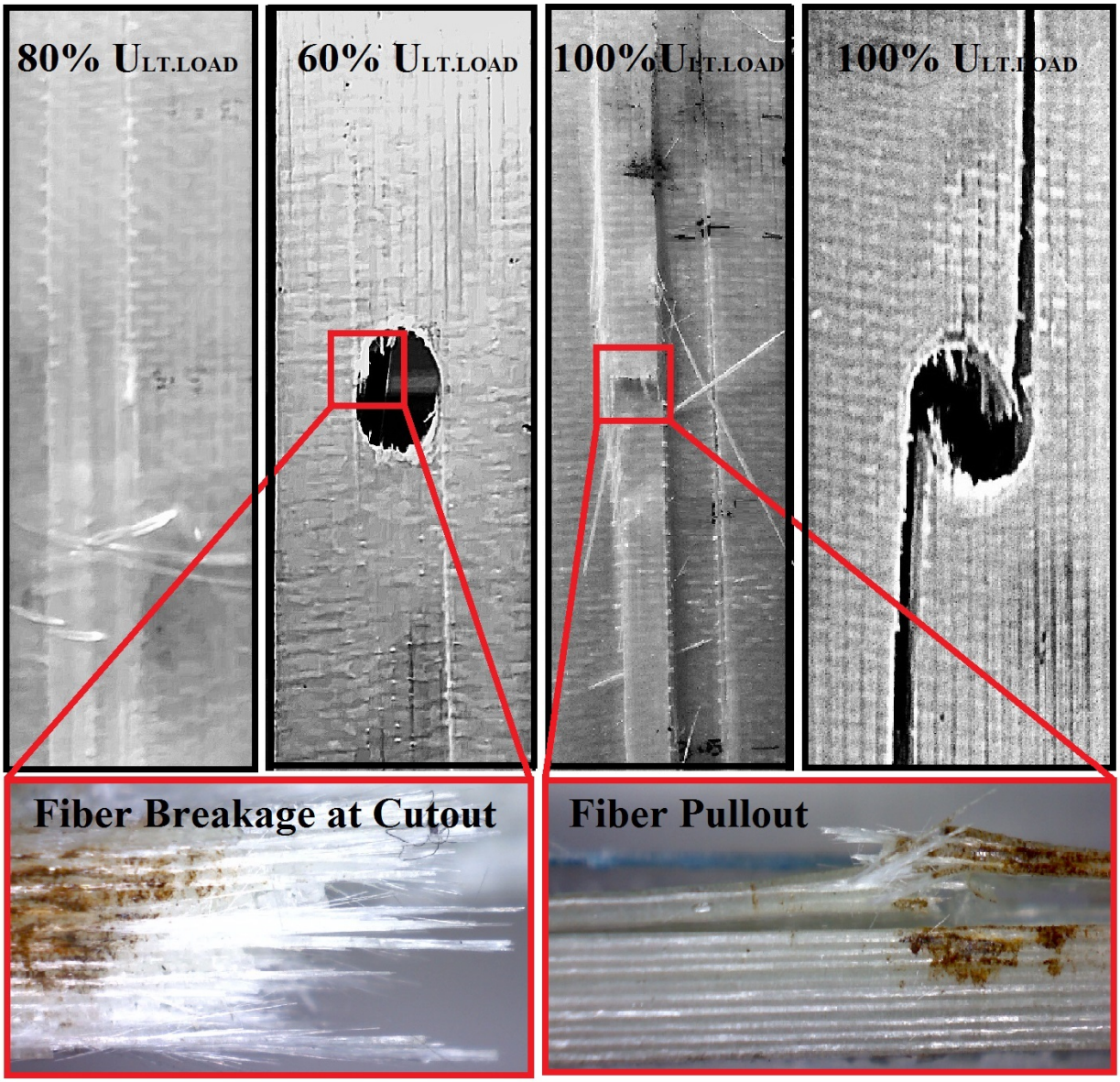

Figure 7 Failure stages of Type I and II laminate

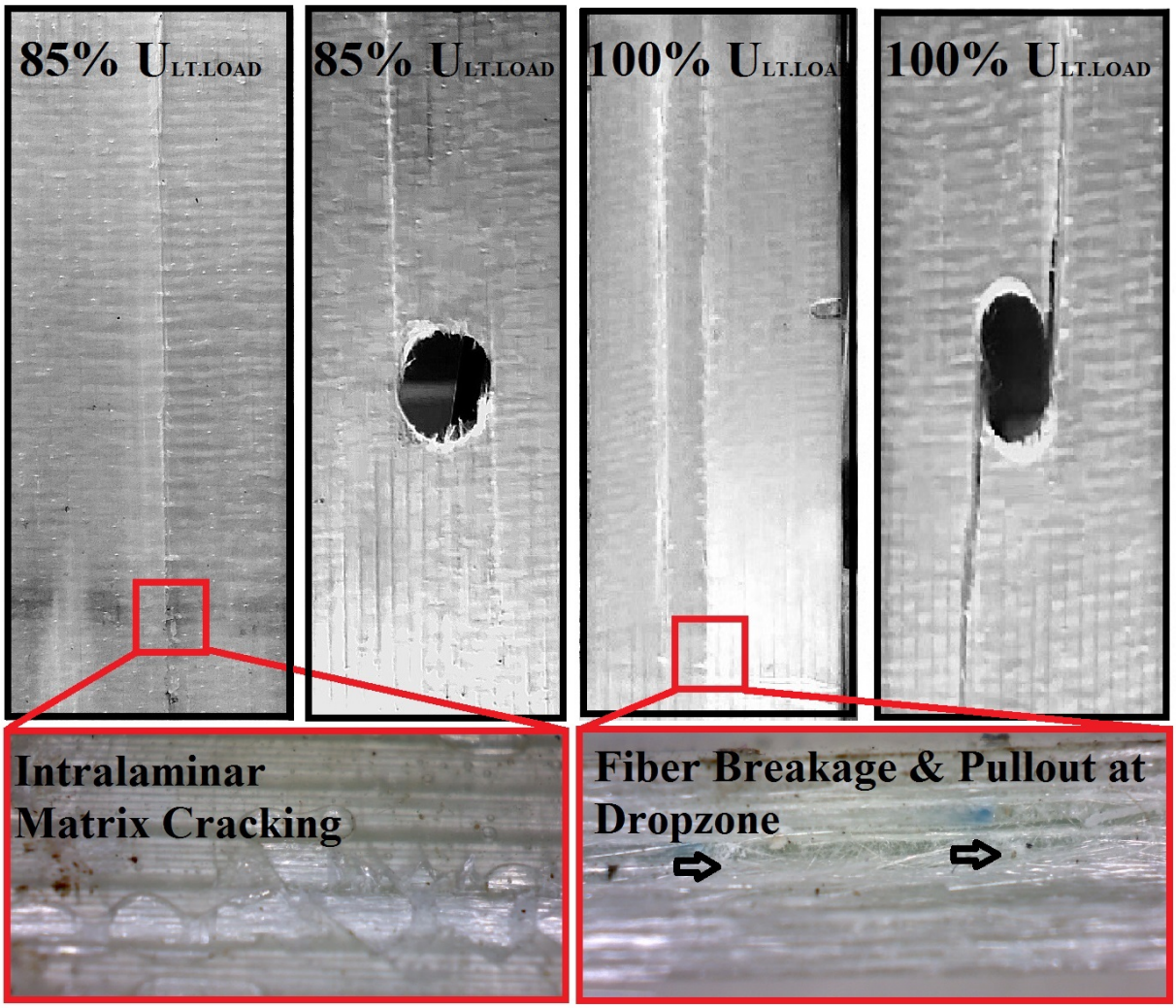

Figure 8 Failure stages of Type III and IV laminate

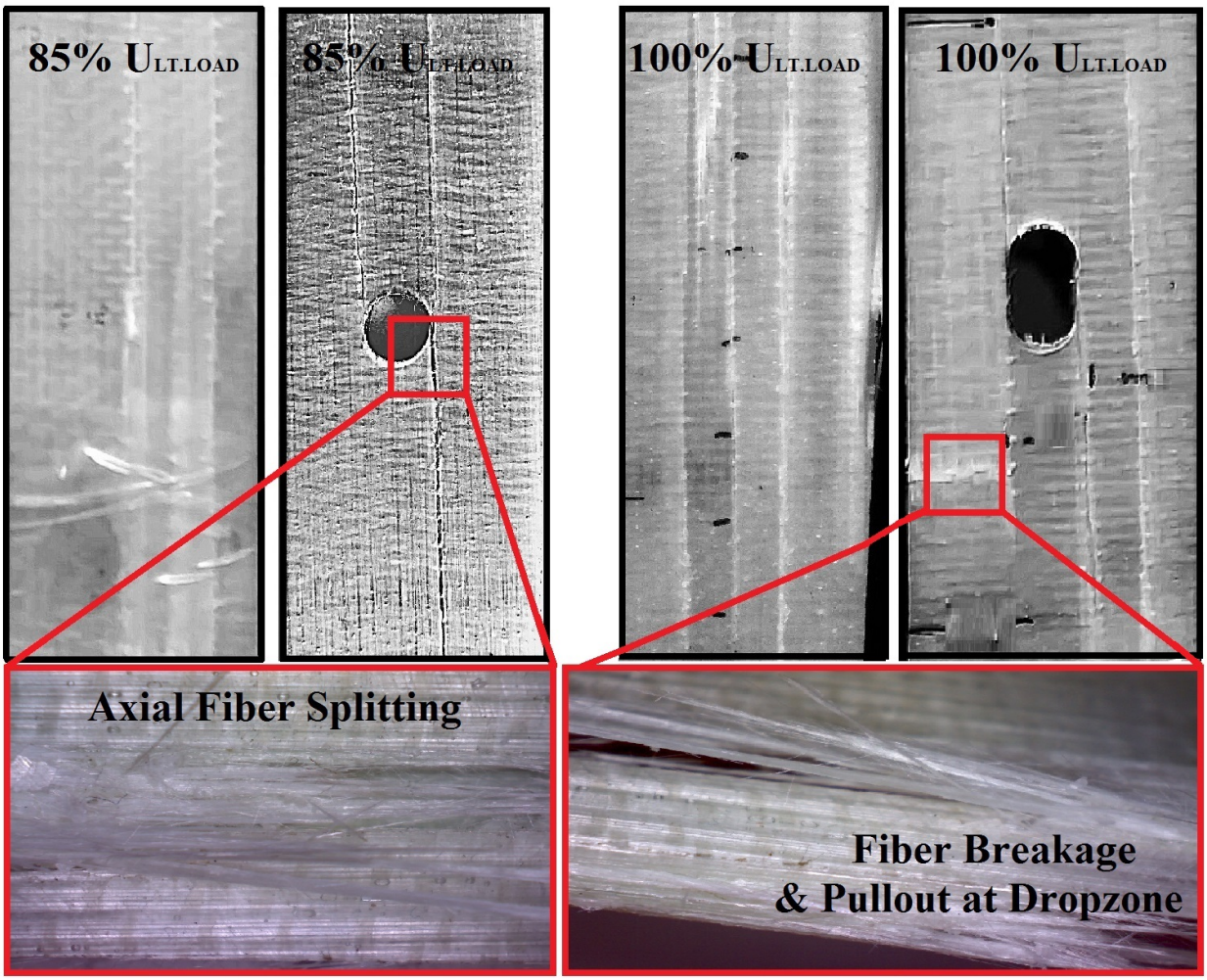

Figure 9 Failure stages of Type V and VI laminate

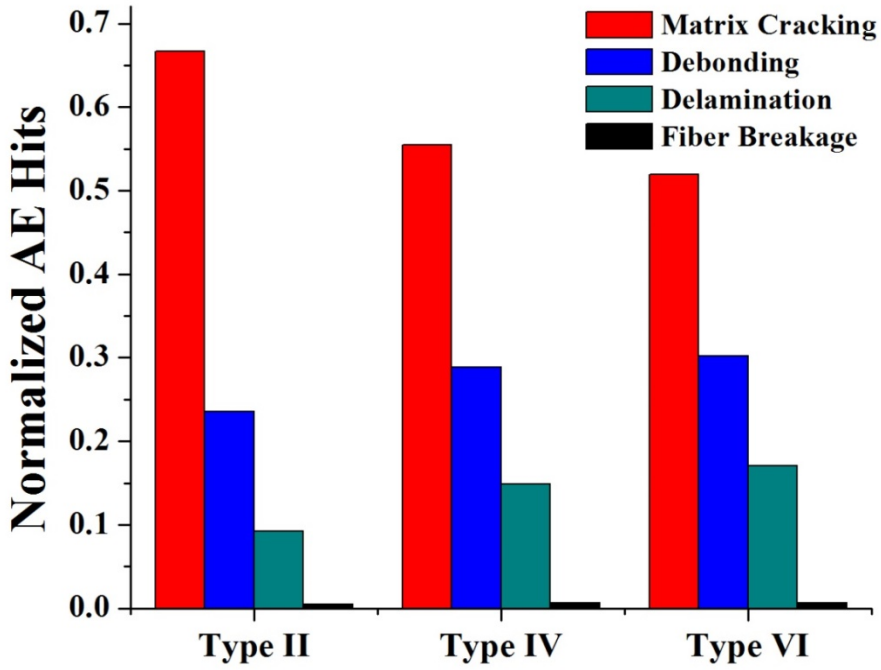

Figure 10. Normalized AE hits for various configurations over the whole of the laminates tested

5. Conclusions

The tensile behavior and failure characteristics of stiffened glass/epoxy laminates with a cut out hole were experimentally investigated with acoustic emission monitoring. Two ply-drop configurations, namely step-like and simultaneous arrangement, were utilized for reinforcing the cutout zones. Reinforcing additional materials at the zones of the cutout was found to be an efficient method to enhance the load carrying capacity and prolongs the damage tolerance of structure. Strength improvement with step-like added plies was demonstrated to be superior than the one obtained with simultaneously added plies, although in no cases the improvement obtained with repair was inferior to 10% of tensile strength. In practice, the creation of holes was obviated by additional ply reinforcements at the zones of cutout hole, delaying the failure at the boundary. However, postponing this failure resulted in stress redistribution through additional ply reinforcements causing an obvious onset of fracture at the junction with ply drop. Acoustic emission technique has been employed as a structural health monitoring tool in stiffened

glass/epoxy composites to characterize the different damage mechanism and to localize the damage. The identification of various damage sources has been performed based on signal frequency and/or amplitude distribution to predict the failure pattern which reflected well in the failure stages of specimens. Thus, the step-like ply arrangements were generally noticed to be more effective in load/strength bearing than simultaneously dropped configurations.

REFERENCES

[1] Gardiner G. Primary structure repair: the quest of quality. High-Performance Composites 2011.

[2] Lee J, Soutis C. Measuring the notched compressive strength of composite laminates: specimen size effects. Composites Science and Technology 68, 2008, 2359–2366.

[3] Pierron F, Green B, Wisnom MR, Hallet SR. Full-field assessment of the damage process of laminated composite open-hole tensile specimens. Part I: Methodology. Composites Part A 38, 2007, 2307–2320.

[4] Pierron F, Green B, Wisnom MR, Hallet SR. Full-field assessment of the damage process of laminated composite open-hole tensile specimens. Part II: Experimental results. Composites Part A 38, 2007, 2321–2332.

[5] Lagattu F, Lafarie-Frenot MC, Lam TQ, Brillaud J. Experimental characterization of over stress accomodation in notched CFRP composite laminates. Composite Structures 67, 2005, 347-357.

[6] Wu H-C, Mu B, On stress concentrations for isotropic/orthotropic plates and cylinders with a circular hole, Composites Part B 34, 2003, 127-134.

[7] Takeda T, Takano S, Shindo Y, Narita F. Deformation and progressive failure behavior of woven fabric-reinforced glass/epoxy composite laminates under tensile loading at cryogenic temperatures. Composites Science and Technology 65, 2005, 1691–1702.

[8] Kaltakci MY. Stress concentrations and failure criteria in anisotropic plates with circular holes subjected to tension or compression. Computers and Structures 61, 1996, 67-78.

[9] Aljibori HS, Chong WP, Mahlia MI, Chong WT, Edi P, Al-Qrimli H, Anjum I, Zahari R. Load–displacement behavior of glass fiber/epoxy composite plates with circular cutouts subjected to compressive load. Materials & Design 31, 2010, 466–474.

[10] Wang J, Callus P, Bannister M. Experimental and numerical investigation of the tension and compression strength of un-notched and notched quasi-isotropic laminates. Composite Structures 64, 2004, 297–306.

[11] Labeas G, Belesis S, Stamatelos D. Interaction of damage failure and postbuckling behaviour of composite plates with cut-outs by progressive damage modelling. Composites Part B 39, 2008, 304–15.

[12] Manoharan R, Jeevanantham AK. Stress and load–displacement analysis of fiber reinforced composite laminates with a circular hole under compressive load. ARPN Journal of Engineering and Applied Sciences 6 (4), 2011, 64–74.

[13] Murat Arslan H, Yasar Kaltakci M, Yerli Huseyin R. Effect of circular holes on cross-ply laminated composite plates. Arabian Journal of Science and Engineering 34, 2009, 301–315.

[14] Camanho PP, Maimi P, Davila CG. Prediction of size effects in notched laminates using continuum damage mechanics. Composite Science and Technology 67, 2007, 2715–2727.

[15] Lee HK, Kim BR. Numerical characterization of compressive response and damage evolution in laminated plates containing a cutout. Composites Science and Technology 67, 2007, 2221–2230.

[16] Chen BY, Tay TE, Baiz PM, Pinho ST. Numerical analysis of size effects on openhole tensile composite laminates. Composites Part A 47, 2013, 52–62.

[17] Hallett SR, Green BG, Jiang WG, Wisnom MR. An experimental and numerical investigation into the damage mechanisms in notched composites. Composites Part A 40, 2009, 613-624.

[18] Wisnom MR, Hallett SR, Soutis C. Scaling effects in notched composites. Journal of Composite Materials 44, 2010, 195–210.

[19] Ridha M, Wang CH, Chen BY, Tay TE. Modelling complex progressive failure in notched composite laminates with varying sizes and stacking sequences. Composites Part A 58, 2014, 16-23.

[20] Maa R-H, Cheng J-H, A CDM-based failure model for predicting strength of notched composite laminates, Composites Part B 33, 2002, 479-489.

[21] Ersin E, Zor M, Arman Y. Hole effects on lateral buckling of laminated cantilever beams. Composites Part B 2009;40:174–9.

[22] Jones RM. Mechanics of composite materials. New York: McGraw-Hill; 1975.

[23] Eiblmeier J, Loughlan J. The buckling response of carbon fibre composite panels with reinforced cut-outs. Composite Structures 32, 1995, 97–113.

[24] Boominathan R, Arumugam V, Santulli C, Adhithya Plato Sidharth A, Anand Sankar R, Sridhar BTN, Acoustic emission characterization of the temperature effect on falling weight impact damage in carbon/epoxy laminates, Composites Part B 56, 2014, 591–598.

[25] Kakakasery J, Arumugam V, Abdul Rauf K, Bull D, Chambers AR, Scarponi C, Santulli C, Cure cycle effect on impact resistance under elevated temperatures in carbon prepreg laminates investigated using acoustic emission, Composites Part B 75, 2015, 298–306.

[26] Grosse CU, Linzer LM. Signal-based AE analysis, in Acoustic emission testing, editors Grosse CU, Ohtsu M, Springer, 2008, ISBN 978-3-540-69895-1.

[27] Barre S, Benzeggagh ML. On the use of acoustic emission to investigate damage mechanism in glass fibre reinforced polypropylene. Composites Science and Technology 52, 1994, 369–376.

[28] Dzenis Y, Qian J. Hybrid transient-parametric AE analysis of histories of damage micro mechanisms in composites. In: Kundu T (ed.) Advanced non-destructive evaluation for structural and biological health monitoring. Vol. 4335 of Proceedings of SPIE, International Society for Optical Engineering, 2001.

[29] Bar HN, Bhat MR, Murthy CRL. Identification of failure modes in GFRP using PVDF sensors: ANN approach. Composite Structures 65, 2003, 231–237.

[30] Berthelot JM, Rhazi J. Acoustic emission in carbon fibre composites. Composites Science and Technology 37, 1990, 411–428.

[31] Chretien JF, Chretien N, A bibliographical survey of acoustic emission. NDT 5, 1972, 220–224.

[32] Hamstad MA, A review: acoustic emission, a tool for composite materials studies. Experimental Mechanics 26, 1986, 7–13.

[33] Yu Y-H, Choi J-H, Kweon, J-H, Kim DH, A study on the failure detection of composite materials using an acoustic emission. Composite Structures 75, 2006, 163–169.

[34] Zhuang X, Yan X, Investigation of damage mechanisms in self-reinforced polyethylene composites by acoustic emission. Composites Science and Technology 66, 2006, 444–449.

[35] Ramirez Jimenez CR, Papadakis N, Reynolds N, Gan TH, Purnell P, Pharaoh M, Identification of failure modes in glass/polypropylene composites by means of the primary frequency content of the acoustic emission event, Composites Science and Technology 64, 2004, 1819–1827.

[36] Arumugam V, Barath Kumar S, Santulli C, Joseph SA, Effect of fiber orientation in uni-directional glass epoxy laminate using acoustic emission monitoring, Acta Metallurgica Sinica (English Letters) 24 (2011) 351–364.

[37] Kotsikos G, Evans JT, Gibson AG, Hale J. Use of acoustic emission to characterize corrosion fatigue damage accumulation in glass fibre reinforced polyester laminates. Polymer Composites 20, 1999, 689–696.

[38] Varughese B, Mukherjee A, A ply drop-off element for analysis of tapered laminated composites, Composite Structures 39, 1997, 123-144.

[39] Munoz V, Valès B, Perrin M, Pastor ML, Welemane H, Cantarel A, Karama M, Damage detection in CFRP by coupling acoustic emission and infrared thermography, Composites Part B 85, 2016, 68–75.

[40] de Groot PJ, Wijnen PAM, Janssen RBF, Real-time frequency determination of acoustic emission for different fracture mechanisms in carbon/epoxy composites, Composites Science and Technology 55 (4), 1995, 405-412.

[41] Petrucci R, Santulli C, Puglia D, Nisini E, Sarasini F, Tirillò J, Torre L, Minak G, Kenny JM, Impact and post-impact damage characterisation of hybrid composite laminates based on basalt fibres in combination with flax, hemp and glass fibres manufactured by vacuum infusion, Composites Part B 69, 2015, 507-515.